Water Practice & Technology

IWA PUBLISHING

Water Practice & Technology Vol 18 No 11, 2664 doi: 10.2166/wpt.2023.176

Photocatalytic and antioxidant potential of silver nanoparticles biosynthesized using *Artemisia stelleriana* leaf extracts

Juhi Puthukulangara Jaison and Joseph Kadanthottu Sebastian *

Department of Life Sciences, Christ University, Bangalore 560029, India
*Corresponding author. E-mail: joseph.ks@christuniversity.in

JPJ, 0009-0008-8426-2345; JKS, 0000-0003-4384-2462

ABSTRACT

The antioxidant and photocatalytic activity of *Artemisia stelleriana*-based silver nanoparticles (AS-AgNPs) was investigated in this study. Microscopic, X-ray diffraction and spectroscopic studies were used to characterize the synthesized AS-AgNPs. UV–visible spectrophotometric examination revealed a peak at 425 nm. The phytocompounds involved in the transformation of silver ions into AS-AgNPs were confirmed using Fourier-transform infrared spectroscopy analysis. The crystalline nature of the AS-AgNPs was verified using the X-ray powder diffraction technique. Spherical-shaped AS-AgNPs with a size of 22.7 nm were proved using field emission scanning electron microscopy. The AS-AgNPs were top-notch photocatalysts for the degradation of Reactive Blue-222A (RB-222A) and Reactive Blue-220 (RB-220) dyes. After 80 min of UV light exposure, AS-AgNPs degraded RB-222A and RB-220 dyes by 94.6 and 90.8%, respectively. The phytotoxicity investigation in *Vigna radiata* and *Artemia salina* indicated that the hazardous dye can be degraded into innocuous chemicals by AS-AgNPs. The results suggest that AS-AgNPs are an excellent antioxidant and photocatalyst for the degradation of synthetic dyes.

Key words: AgNPs, antimicrobial, antioxidant, *Artemisia stelleriana*, degradation, photocatalytic

HIGHLIGHTS

- Silver nanoparticles (AgNPs) were synthesized using *Artemisia stelleriana* leaves.
- Spherical-shaped AgNPs with 22.7 nm size were detected.
- Degradations of Reactive Blue-220 and Reactive Blue-222A dyes were validated owing to the photocatalytic activity of AgNPs.
- Low toxicity was observed during the toxicity analysis of the degraded dye.
- AgNPs also showed significant antioxidant potential.

GRAPHICAL ABSTRACT

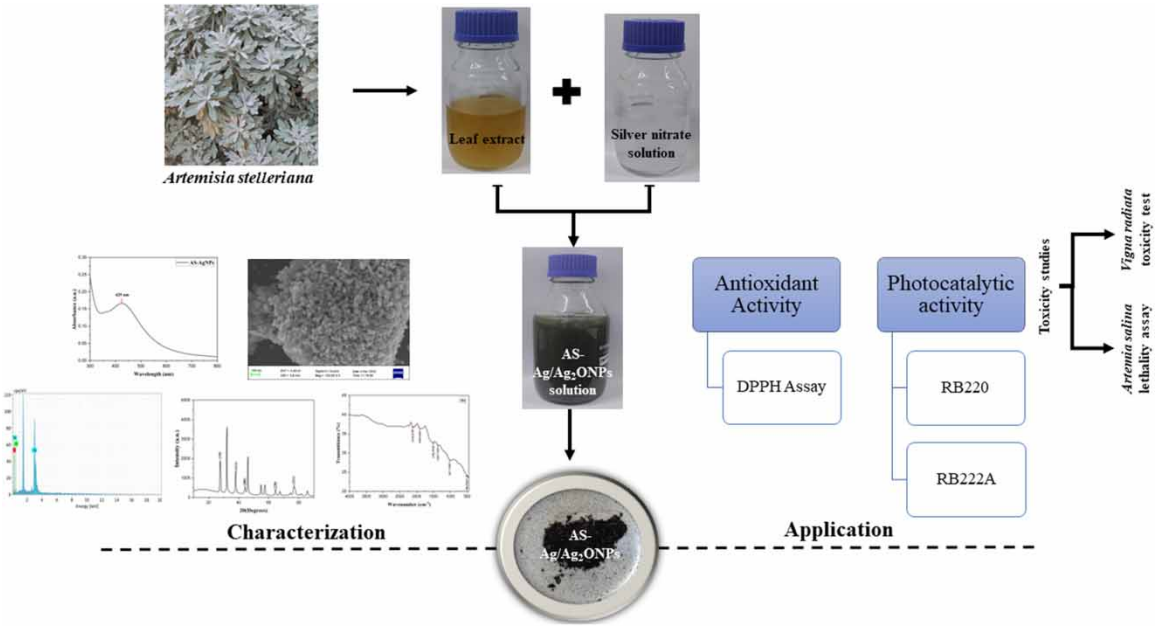

INTRODUCTION

The pharmacological values of plants are the reason for their utilization in treating various infections or diseases from the former age (Sofowora *et al.* 2013). Plants are utilized in multiple fields due to their excellent properties (Prabhu & Poulose 2012). Green synthesis is a part of nanotechnology where plants are widely used as reducing, capping and stabilizing agents (Hussain *et al.* 2016). The plant extract which contains numerous phytochemical compounds can reduce the metal ions to metal/metal oxide nanoparticles (NPs) (Kumar *et al.* 2021). Utilization of plant extract in NP synthesis is an alternative to chemical and physical synthesis (Beyene *et al.* 2017). Plant extract-based NP synthesis is pollution-free, non-toxic, more sustainable and eco-friendlier (Ying *et al.* 2022). One to a hundred nanosized particles have promising activities like antioxidant, antimicrobial, anticancer, anti-diabetic, cytotoxic, anthelminthic, and photocatalytic activities.

Silver nanoparticles (AgNPs) have been reported for different medical properties, so it is used as an alternative medicine for numerous health conditions (Danish *et al.* 2022). It is also reported for other applications like bio-sensing and photocatalytic activities. AgNPs can remove or degrade the dyes utilized in different industries (Prasher & Sharma 2023). The distinct size, shape, and surface characteristics of AgNPs are responsible for their degrading activity. The precise catalytic mechanism of AgNPs in different reactions can vary, although it frequently entails reactant molecule adsorption on the nanoparticle surface, followed by processes for electron transfer (Levard *et al.* 2012).

Artemisia stelleriana is an aromatic herb commonly known to be old women, dusty miller and beach wormwood due to its physical appearance. The plant contains compounds like flavonoids, alkaloids, monoterpenes, sesquiterpenes, vitamins, minerals and other compounds, so it has high medicinal importance. The *A. stelleriana* leaves were utilized in treating peptic ulcers and hair loss. It was also reported that the leaf extract of *A. stelleriana* has good antioxidant activity (Mayuri *et al.* 2022). *A. stelleriana* belongs to the Asteraceae family and has been already reported for synthesizing ZnO NPs which has great photocatalytic activities (Puthukulangara Jaison & Kadanthottu Sebastian 2023).

The present study deals with the green synthesis of AgNPs from the leaf extract of *A. stelleriana*. Green-synthesized NPs were characterized using UV–Visible spectrophotometry (UV–Vis), X-ray diffraction (XRD), Fourier-transform infrared spectroscopy (FTIR), energy-dispersive X-ray spectroscopy (EDX), and field emission scanning electron microscopy (FESEM) and their photocatalytic and antioxidant activities. We also attempted to study the toxicity of degraded dyes using *Vigna radiata* and *Artemia salina* lethality assay.

MATERIALS AND METHODS

Plant extract preparation

Healthy leaves of *A. stelleriana* were weighed (10 g) and cleaned with sterile distilled water and were refluxed up to 30 min at 60 °C with 50 ml sterile distilled water and cooled. The extract was filtered using No. 1 Whatman filter paper, and the filtrate was used for the synthesis of AgNPs.

Synthesis of AS-AgNPs

The reduction of silver nitrate was confirmed after the solution mixture changed to brownish black when 50 ml of the *A. stelleriana* extract was added to 400 ml of silver nitrate solution (0.01 M) and made up the volume to 500 ml using sterile distilled water. Then, the mixture was stirred for 2 h at room temperature. The synthesized AgNPs were separated and purified using centrifugation (at 10,000 rpm for 10 min) (Ravichandran *et al.* 2019).

Characterization of AS-AgNPs

The reduction of silver ions to NPs in the extract was verified by a UV–Vis spectrophotometer (300–800 nm) (Shimadzu UV-1800ENG240V UV Spectrophotometer). The surface morphology of the synthesized AS-AgNPs was confirmed by FESEM (ZEISS Sigma HV). The elemental composition and percentage were validated by EDX analysis. The functional groups that helped in the transformation of ions to NPs were studied using FTIR (QATR-S Spectrophotometer) at a resolution of 2 cm^{-1} and scanning range of 500–4,000 cm^{-1}. The crystalline nature and size of the NPs were identified using XRD analysis (Rigaku MiniFlex X-ray Diffractometer).

Photocatalytic activity

The photocatalytic degradation activity of *A. stelleriana*-mediated silver nanoparticles (AS-AgNPs) was evaluated by RB-220 and RB-222A dye degradation in the presence of AS-AgNPs under UV (~253.7 nm) (Philips TUV 30W 1SL/25 T8 UV Lamp) light exposure. Approximately 5 mg/L of dyes was used in this experiment. About 1 mg/ml of AS-AgNPs was dispersed in distilled water by sonication. The dye solution was mixed with sonicated AS-AgNPs solution magnetically stirred for 10 min in the dark and then exposed to UV light. At specific time intervals, 3 ml of suspension was collected and centrifuged to remove the NPs from the sample solution. The sample solution was examined spectrophotometrically to study the degradation of dyes from 200 to 800 nm and the photocatalytic degradation efficiency of AS-AgNPs was determined using the equation:

$$\text{Percentage of degradation} = (\text{Initial absorbance} - \text{Final absorbance})/\text{Final absorbance} \times 100 \quad (1)$$

Scavenger studies

Similar to photocatalytic degradation, scavenging studies were determined. Along with the catalyst, 0.01 mmol of isopropyl alcohol (IPA), 0.1 mmol of ascorbic acid (AA), and 0.01 mmol of ethylenediaminetetraacetic acid (EDTA) were added to the dye to scavenge hydroxyl radicals (OH^-), superoxide radicals (O_2^-) and holes (h^+), respectively.

Toxicological studies

The degradation efficiency of AS-AgNPs and treated dye phytotoxicity reduction were determined using the *V. radiata* toxicity test and *A. salina* lethality assay. *V. radiata* toxicity test was performed as the previously reported method with minor changes (Dharshini *et al.* 2023; Puthukulangara Jaison & Kadanthottu Sebastian 2023). The *V. radiata* seeds were allowed to germinate in a Petri dish and subjected to untreated and treated dye solutions, respectively. After 7 days of treatment, the plant's root and shoot length toxicity were evaluated. *A. salina* (Brine shrimp) lethality assay was studied using an already described protocol with minor modifications (Bilal *et al.* 2016). In test tubes, the hatched nauplii (10 each) were exposed to untreated and treated dye solutions for 24 h and then the mortality rate (MR) was evaluated by counting the dead nauplii under a binocular microscope.

In-vitro antioxidant assay

The antioxidant property of the synthesized AS-AgNPs was examined using a 2,2′-diphenyl-1-picrylhydrazyl (DPPH) assay with minor changes. The DPPH solution was freshly made by dissolving 4 mg DPPH with 100 ml of 80% methanol. The stock solution of AA and AS-AgNPs was prepared in 1 mg/ml concentrations. Approximately 100 µl of the test sample solution at various concentrations (1–100 µg/ml) was taken and made

up to 3 ml with 80% methanol. One millilitre of freshly prepared DPPH solution was added to all the test solutions and incubated in a dark condition for 30 min. In the UV–Vis spectrophotometer, the absorbance of the samples was taken at 517 nm. The blank was 80% methanol and the control was without the test sample solution. The free radical scavenging activity was confirmed based on the percentage of the DPPH radical scavenged as the following equation (Zhang *et al.* 2022):

$$\text{DPPH scavenged (\%)} = (\text{Absorbance}_{\text{control}} - \text{Absorbance}_{\text{standard}})/\text{Absorbance}_{\text{control}} * 100 \quad (2)$$

RESULTS AND DISCUSSION

Synthesis and UV–Vis spectral analysis

NPs synthesis starts once the *A. stelleriana* leaf extract is mixed with the silver nitrate solution. The solution colour turned from pale yellow to brownish black was the initial confirmation of the synthesis of NPs. Surface plasmon vibration is the reason for this colour change and it is an optical character that is unique for all noble metals (Rautela *et al.* 2019). The UV–Vis spectra of AS-AgNPs colloidal solution were recorded from 200 to 800 nm, with a peak at 425 nm (Figure 1(a)), which confirms the existence of silver/silver oxide NPs. A similar kind of result was observed in AS-AgNPs synthesized using *Artemisia herba-alba* and *Eupatorium odoratum* (Elemike *et al.* 2017; Belaiche *et al.* 2021).

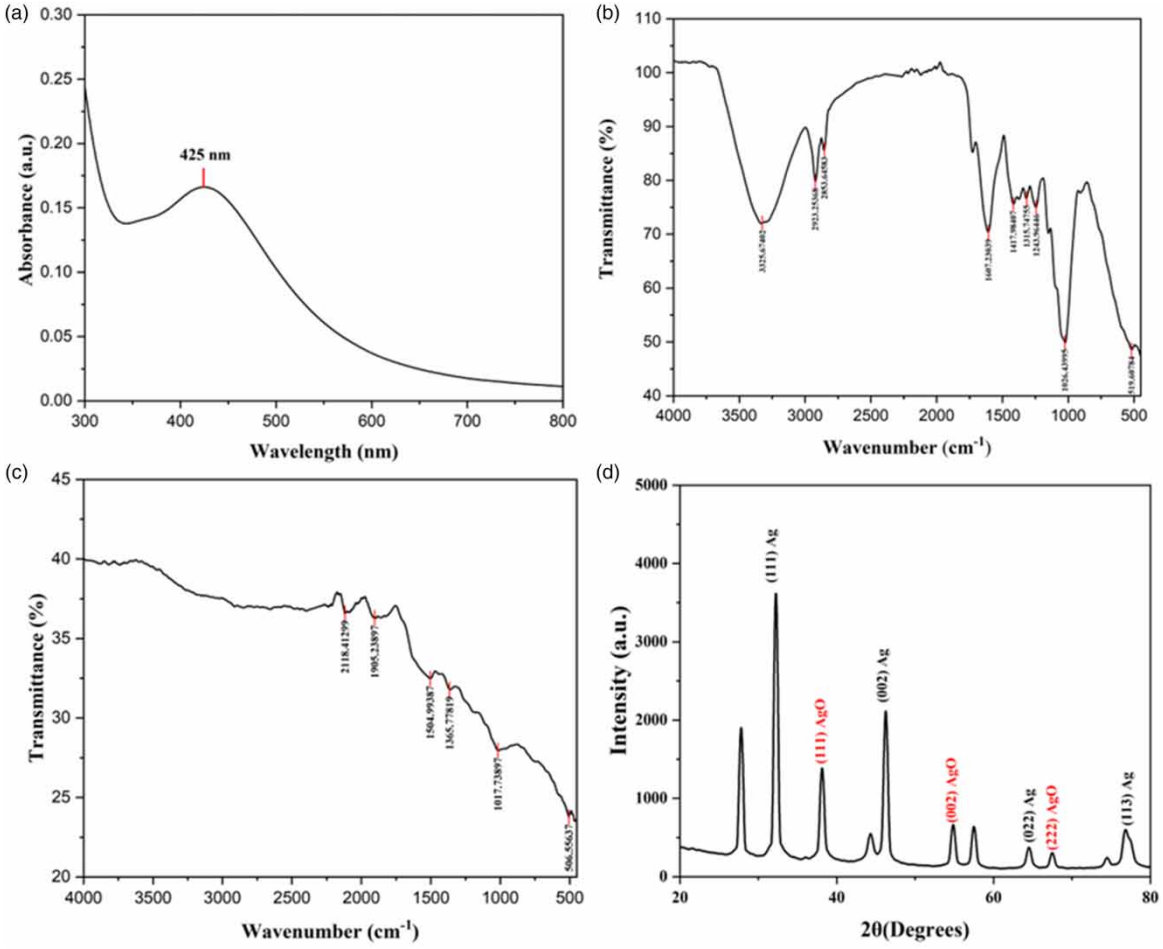

Figure 1 | (a) UV–Vis spectrum showing Surface plasmon resonance (SPR) peak, FTIR spectra of (b) plant extract, (c) synthesized nanoparticle and (d) XRD pattern of Ag/AgONPs synthesized from *Artemisia stelleriana* leaves.

Fourier-transform infrared spectroscopy (FTIR)

The FTIR spectrum helps to confirm the functional groups involved in the stabilization and reduction of Ag ions to NPs. The FTIR spectrum of *A. stelleriana* extract and synthesized AS-AgNPs was noticed from the range

between 500 and 4,000 cm^{-1}. The figure shows the FTIR spectral analysis of the leaf powder of *A. stelleriana* (Figure 1(b)) and AS-AgNPs (Figure 1(c)). The FTIR spectrum of *A. stelleriana* leaf powder exhibited multiple peaks at 3,325.67, 2,923.25, 2,853.64, 1,607.23, 1,417.98, 1,315.74, 1,243.96, 1,026.43 and 519.60 cm^{-1}. The peaks at 3,325.67 and 2,923.25 cm^{-1} (O–H stretching), 2,853.64 cm^{-1} (N–H stretching), 1,607.23 cm^{-1} (C = C stretching), 1,417.98 and 1,315.74 cm^{-1} (O–H bending), 1,243.96 cm^{-1} (C–O stretching), 1,026.43 cm^{-1} (CO–O–CO stretching) and 519.60 cm^{-1} (C–Br stretching) may be associated with tannins, flavonoids, alkaloids, resins, saponins and phenolic compounds present in the *A. stelleriana* extract (Mousavi *et al.* 2018). The bio-synthesized AS-AgNPs showed bands at 2,118.41 cm^{-1} (C ≡ C stretching), 1,905.23 cm^{-1} (C = C = C stretching), 1,504.99 cm^{-1} (N–O stretching) 1,365.77 cm^{-1} (O–H bending) and 1,017.73 cm^{-1} (C–F stretching). The metal-oxygen bond is ascribed to the peaks at 506.55 cm^{-1}, confirming the synthesis of AS-AgNPs. The reduction in O–H bands and the appearance of carboxyl groups after AS-AgNPs formation could be symptomatic of redox reactions between Ag ions and biomolecules. The electron in the carbonyl group can be a reason for the transformation of Ag ions to AS-AgNPs (Laouini *et al.* 2021).

X-ray diffraction (XRD)

The identified diffraction pattern revealed the crystalline nature of synthesized *A. stelleriana*-based AS-AgNPs, as shown in Figure 1(d). According to the Debye-Scherrer formula:

$$D = \frac{K\lambda}{\beta \cos\theta} \tag{3}$$

where D is the crystallite size of nanoparticles, λ is the wavelength of the X-ray source, β is the 'full width at half maximum' of the diffraction peak, K is the Scherrer constant and θ is the Bragg angle. The synthesized AS-AgNPs have an average crystalline size of 18.67 nm and the distinctive peaks observed at 2θ values of 38.1°, 44.3°, 64.3° and 77.0° were matched to the planes of Ag, i.e., (111), (002), (022) and (113) reflection of the face-centred cubic structure of AgNPs (JCPDS cards# 98-005-0882). Additionally, peaks at 32.3°, 54.9° and 67.4° were observed, indicating the presence of silver oxide NPs, with lattice planes identified as (111), (022) and (222) which correspond with JCPDS cards# 98-001-4796. A comparable observation was found in Ag/AgONPs synthesized using *Crocus sativa* leaf extract (Abdalameer *et al.* 2021).

Field emission scanning electron microscopy (FESEM) and energy-dispersive X-ray spectroscopy (EDX)

The morphology and elemental analysis of the AS-AgNPs were evaluated using FESEM and EDX analysis. FESEM analysis displayed spherical-shaped AS-AgNPs with 22.7 nm in size (Figure 2(a)). The EDX data showed the synthesized AS-AgNPs consist of elements such as silver (38.18%), oxygen (53.19%) and carbon (8.63%) (Figure 2(b)). Since the percentage of oxygen in EDX analysis is 53.19 both silver and silver oxide NPs can be formed. The spectra showed peaks in the range of 2–4 keV for silver which are distinctive for AgNPs as reported in AgNPs synthesized from *Artemisia nilagirica* (Vijayakumar *et al.* 2013).

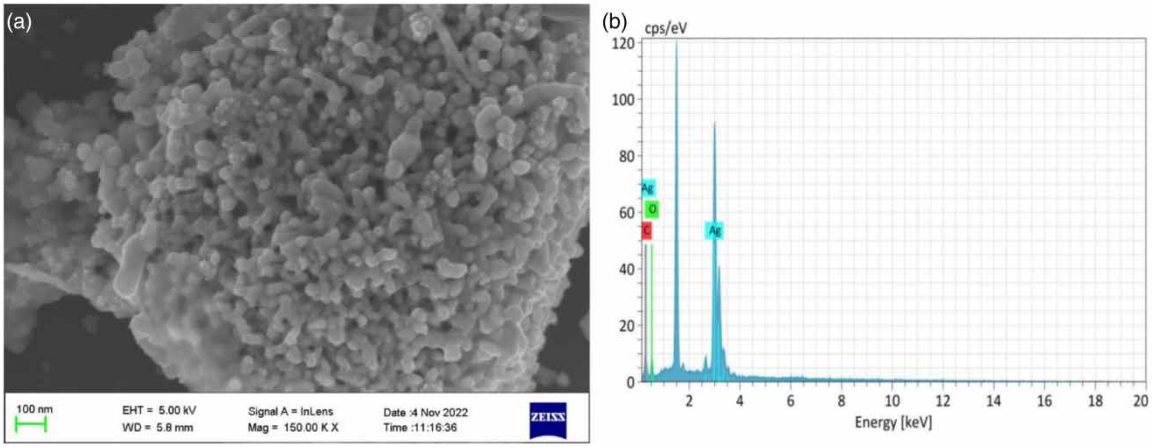

Figure 2 | Characterization of biogenic AS-AgNPs by (a) SEM analysis and (b) EDX.

Photocatalytic activity

AS-AgNP-mediated photocatalytic degradation was analyzed using RB-222A and RB-220 dyes. At specific time intervals (0, 10, 20, 40 and 80 min), the degradation percentage was noted and it was observed that at 80 min, the percentage of degradation in RB-220 and RB-222A was 90.8% (Figure 3(a)) and 94.6% (Figure 3(b)), respectively. There was a gradual decrease in the intensity of the dye colours with time. The primary causes of dye decolourization were hydroxyl and oxy radicals, which break down hazardous pollutants generated when a hole–electron pair is formed. When compared to a recent study that used biosynthesized cobalt oxide NPs for RB-220 dye degradation (67%), our results were superior (Valappil *et al.* 2019). Another study found that *Artemisia annua*-mediated silver NPs can degrade dyes (Adoni *et al.* 2020).

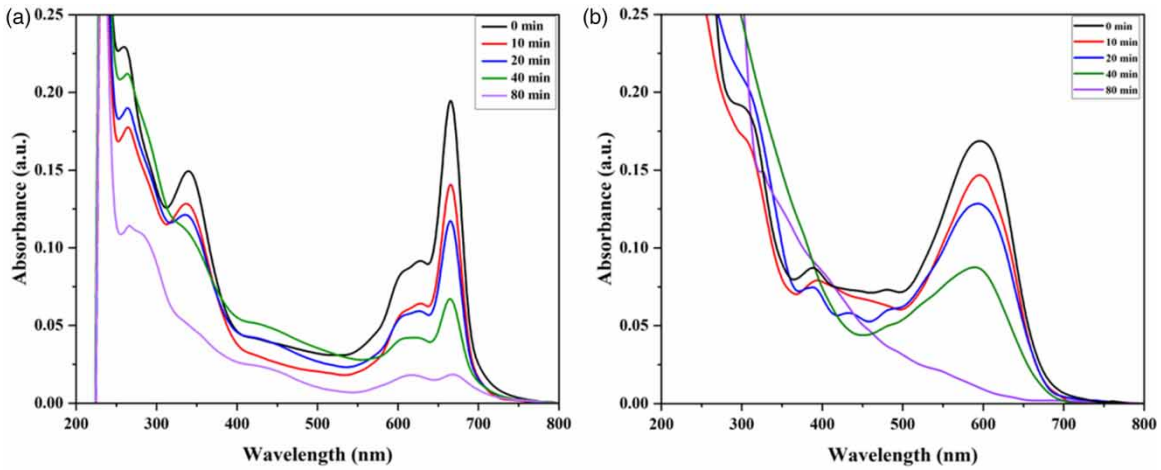

Figure 3 | Photocatalytic degradation of dyes at different time intervals (0–80 min) (a) Reactive Blue-220 (RB-220) and (b) Reactive Blue-222A (RB-222A).

Kinetic studies

Kinetic studies were conducted using the following relationship to determine the degradation rate of dye molecules under ideal conditions:

$$-\ln A_t/A_0 = kt \tag{4}$$

where A_t is the absorbance of dye at time, t, A_0 is the absorbance of dye at time $t = 0$ and k is the rate constant. Figure 4(a) represents the plot of A_t/A_0 versus time and Figure 4(b) represents the plot of $-\ln A_t/A_0$ versus time. The rate of degradation was greatly increased by the addition of AS-AgNPs as a catalytic agent in the dye solution, reaching 0.0293 and 0.0164 min^{-1} for RB-220 and RB-222A (Figure 4). The slope of the curve shows the sequence of the reaction (first-order kinetics due to dye degradation).

Scavenger studies

It is interesting to note that the breakdown of the dye was mostly influenced by holes and hydroxyl radicals. The degradation process of the dye was unaffected by the addition of AA, a superoxide radical scavenger, as can be seen in Figure 5, suggesting that superoxide radicals did not affect the dye's degradation. The least amount of dye degradation occurred when the hole scavenger EDTA was used, and the addition of IPA to the dye degraded it even less. This indicates that the hydroxyl radical and holes directly affected the degradation process.

It is possible that under UV light, electrons will get excited from the valence band to the conduction band which leads to the formation of photogenerated species, i.e., a positive hole in the valance band and conduction electrons in the conduction band. These photogenerated species help in the degradation of RB-220 and RB-222A dyes by developing highly reactive radicles. By interacting with water molecules, the positive holes create the hydroxyl group and hydrogen ion, which are then transformed into hydroxyl radicals. Meanwhile, the dissolved oxygen interacts with the water molecule to create the hydroxyl radical. In photocatalytic degradation, these photogenerated radicals, i.e., hydroxyl radicals and holes, play a crucial role (Shaikh *et al.* 2020; Bhatt & Patel 2021).

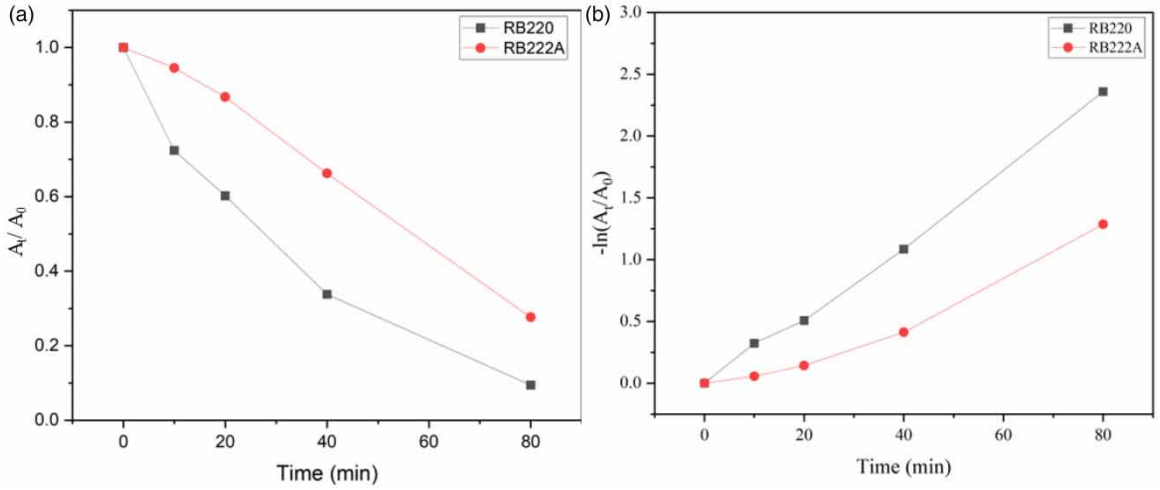

Figure 4 | Kinetic results of dye degradation (a) A_t/A_0 versus time and (b) $-\ln A_t/A_0$ versus time.

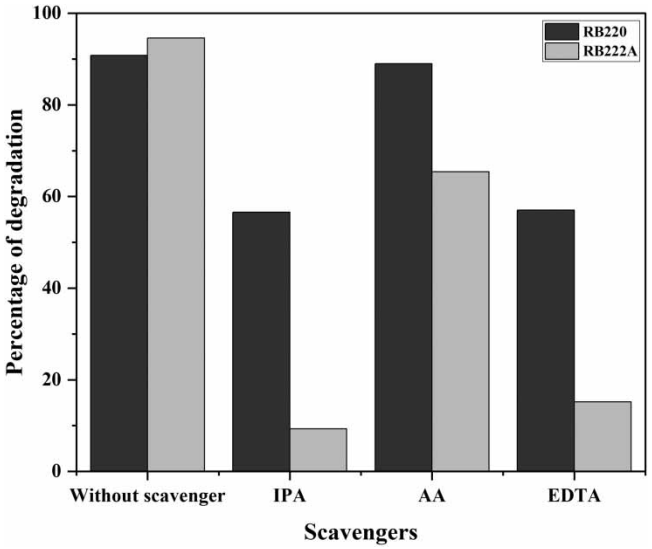

Figure 5 | Scavenger studies for AS-AgNPs against Reactive Blue-220 (RB-220) and Reactive Blue-222A (RB-222A).

Reusability of AS-AgNPs

The reusability of AS-AgNPs is their key selling point. Centrifugation was used to separate the solid catalyst from the reaction mixture, and it was then washed with methanol to remove any extra starting material or product from its surface and dried for 30 min at 60 °C. The recovered catalyst was used in other processes. The AS-AgNPs were found to be fairly usable up to three consecutive reactions, but the fourth cycle reaction resulted in a significantly lower percentage of degradation (Figure 6) which may be due to the subsequent loss of NPs during the reaction or recovery process. XRD data of AS-AgNPs utilized in the dye degradation was observed, the crystalline nature of AS-AgNPs was not changed after the degradation of dyes and the peak position also remained be same as before the degradation for RB-220 and RB-222A (Figure 7(a) and 7(b)). The observation concluded that the AS-AgNPs are stable and reusable. These are in concurrence with the previous reports (Chikkanayakanahalli Paramesh *et al.* 2021).

Toxicity study

Toxicity studies showed traceable changes after treatment with AS-AgNPs in *V. radiata* and *A. salina*. The phytotoxicity investigation was done using *V. radiata* which have great relevance in the food industry. The growth of

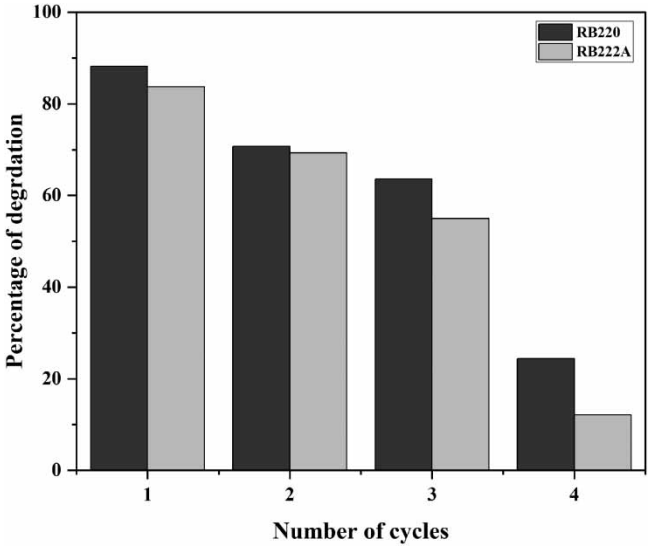

Figure 6 | Reusability of AS-AgNPs as photocatalyst.

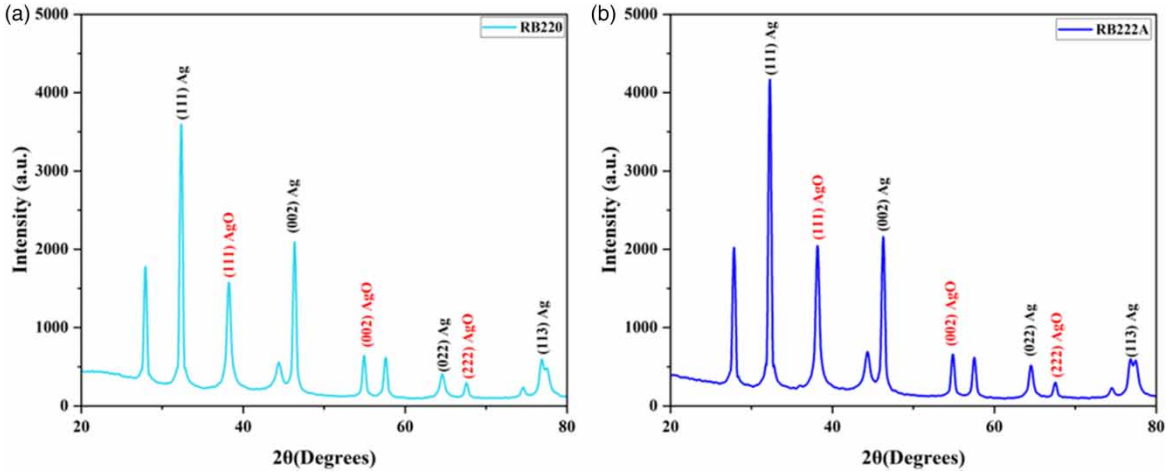

Figure 7 | Characterization of recovered AS-AgNPs by XRD analysis after treatment with different dyes: (a) RB-220 and (b) RB-222A.

shoot and root length of *V. radiata* seeds in untreated textile dyes was suppressed. Seeds cultivated in treated textile dyes, on the other hand, grew faster in terms of shoot and root length. Root length increased by 78.1 and 87.8% for treated water with RB-220 and RB-222A dyes, respectively, and shoot length grew by 74.3 and 66.1% for treated water with RB-220 and RB-222A dyes, respectively (Figure 8(a)). In *V. radiata* toxicity test, it was deduced that phytotoxicity reduced vastly after dye treated with AS-AgNPs. In the current study, the treated solution did not indicate any toxicity; it showed that the harmful substances in the dyes were reduced or degraded to non-toxic compounds through biodegradation.

Brine shrimp (*Artemia salina*) is a model organism for toxicity studies that are true representative of aquatic life. The brine shrimp lethality test was done to know the ability to kill brine shrimp nauplii hatched in the laboratory within a certain period. After one day, it was noticed that all the brine shrimp remained alive in the artificial seawater, and in potassium permanganate solution, all nauplii were dead. It was also observed that the MR was lower in the treated effluents in comparison with the untreated effluents. When compared with all the treated samples, the maximum MR was noticed in RB-222A dye and the least mortality was observed in RB-220 dye (Figure 8(b)). The current investigation proved that Ag/Ag_2ONPs synthesized from the

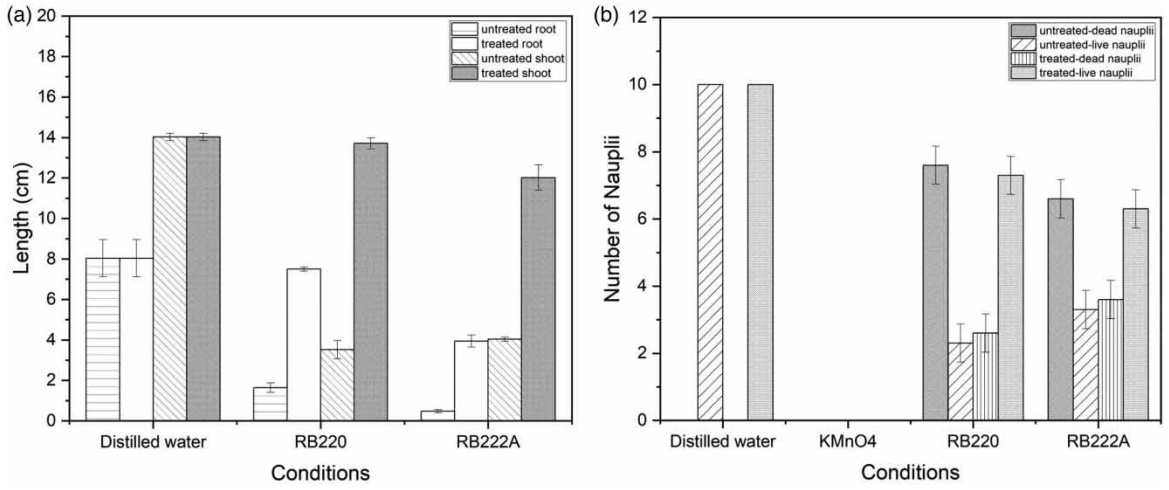

Figure 8 | Toxicity assessment of untreated and treated textile dyes: (a) *V. radiata* and (b) *A. salina*.

A. stelleriana degraded the toxic compounds from textile dyes. ZnO NPs synthesized for *A. stelleriana* also displayed similar effects nullifying the effects of toxic dyes through brine shrimp assay and *V. radiata* tests (Puthukulangara Jaison & Kadanthottu Sebastian 2023).

Antioxidant activity

Earlier findings reported that green-synthesized AS-AgNPs have promising antioxidant activity. AgNPs undergo oxidation to neutralize the free radical formed (Mittal *et al.* 2012). Here, the antioxidant activity of AS-AgNPs was determined by DPPH radical scavenging activity. The AA was utilized as standard. The antioxidant activity of the test solution was raised with increasing concentrations of AS-AgNPs in the range of 100–600 μg/ml resulting in a rise in the percentage of DPPH radical scavenging activities. When the dosage of AS-AgNPs is increasing, the scavenging activity also increases in a dose-dependent pattern. The highest radical scavenging activity exhibited at 600 μg/ml of AS-AgNPs (76.3%). The IC_{50} value of AS-AgNPs was 105 μg/ml (Figure 9). Ag NPs synthesized from *Artemisia absinthium* have significant antioxidant properties against DPPH assay (Balciunaitiene *et al.* 2021). Free radical scavenging activity was also observed in *Artemisia afra*-mediated Ag NPs (Elemike *et al.* 2018).

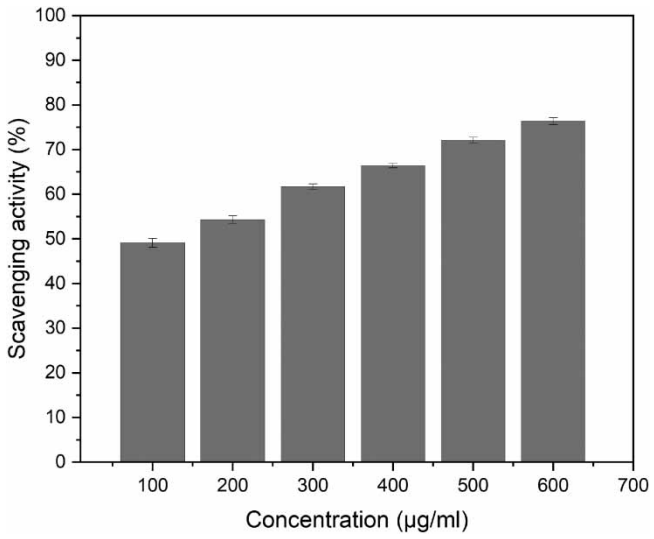

Figure 9 | Antioxidant activity of AgNPs synthesized from *A. stelleriana* leaves.

CONCLUSION

The *A. stelleriana* leaf extract-mediated AS-AgNPs were synthesized and characterized using spectroscopic and microscopic analyses. The protocol adopted here is a cost-effective, simple, non-toxic and pollution-free method. Spherical-shaped Ag/Ag_2ONPs with an average size of 22.7 nm were synthesized. The radical scavenging activity was observed at 600 μg/ml of AS-AgNPs. Under UV light irradiation, the synthesized NPs showed the degradation of toxic industrial dyes, RB-220 and RB-222A. The toxicity study conducted in *V. radiata and A. salina* also revealed that the Ag/Ag_2ONPs synthesized from *A. stellariana* successfully reduced the toxicity of the textile dyes. The limitation of this study was that the complete recovery of NPs was not possible. The study can be further extended by developing nanomembranes or nanocapsules using AS-AgNPs, which can be utilized in the degradation of hazardous textile dyes. Future research on the production of nanomembranes or nanocapsules and their applications in both environmental and biomedical fields can be guided by the findings of this study.

DATA AVAILABILITY STATEMENT

All relevant data are included in the paper or its Supplementary Information.

CONFLICT OF INTEREST

The authors declare there is no conflict.

REFERENCES

Abdalameer, N. K., Khalaph, K. A. & Ali, E. M. 2021 Ag/AgO nanoparticles: Green synthesis and investigation of their bacterial inhibition effects. *Materials Today: Proceedings* **45**, 5788–5792.

Adoni, M., Yadam, M., Gaddam, S. A., Rayalacheruvu, U. & Kotakadi, V. S. 2020 Antimicrobial, antioxidant, and dye degradation properties of biosynthesized silver nanoparticles from *Artemisia annua* L. *Letters in Applied NanoBioScience* **10**, 1981–1992.

Balciunaitiene, A., Viskelis, P., Viskelis, J., Streimikyte, P., Liaudanskas, M., Bartkiene, E., Zavistanaviciute, P., Zokaityte, E., Starkute, V., Ruzauskas, M. & Lele, V. 2021 Green synthesis of silver nanoparticles using extract of *Artemisia absinthium* L., *Humulus lupulus* L. and *Thymus vulgaris* L., physico-chemical characterization, antimicrobial and antioxidant activity. *Processes* **9**(8), 1304.

Belaiche, Y., Khelef, A., Salah Eddine, L., Abderrhmane, B., Tedjani, M. & Barhoum, A. 2021 Green synthesis and characterization of silver/silver oxide nanoparticles using aqueous leaves extract of *Artemisia herba-alba* as reducing and capping agents. *Revista Romana de Materiale=Romanian Journal of Materials=RRM* **51**, 342–352.

Beyene, H. D., Werkneh, A. A., Bezabh, H. K. & Ambaye, T. G. 2017 Synthesis paradigm and applications of silver nanoparticles (AgNPs), a review. *Sustainable Materials and Technologies* **13**, 18–23.

Bhatt, D. K. & Patel, U. D. 2021 Photocatalytic degradation of Reactive Black 5 using Ag_3PO_4 under visible light. *Journal of Physics and Chemistry of Solids* **149**, 109768.

Bilal, M., Iqbal, M., Hu, H. & Zhang, X. 2016 Mutagenicity, cytotoxicity and phytotoxicity evaluation of biodegraded textile effluent by fungal ligninolytic enzymes. *Water Science and Technology* **73**, 2332–2344.

Chikkanayakanahalli Paramesh, C., Halligudra, G., Gangaraju, V., Sriramoju, J. B., Shastri, M., Kachigere B, H., Habbanakuppe D, P., Rangappa, D., Kanchugarakoppal Subbegowda, R. & Doddakunche Shivaramu, P. 2021 Silver nanoparticles synthesized using saponin extract of *Simarouba glauca* oil seed meal as effective, recoverable and reusable catalyst for reduction of organic dyes. *Results in Surfaces and Interfaces* **3**, 100005.

Danish, M. S. S., Estrella-Pajulas, L. L., Alemaida, I. M., Grilli, M. L., Mikhaylov, A. & Senjyu, T. 2022 Green synthesis of silver oxide nanoparticles for photocatalytic environmental remediation and biomedical applications. *Metals* **12**(5), 769.

Dharshini, R. S., Poonkothai, M., Srinivasan, P., Mythili, R., Syed, A., Elgorban, A. M. & Kim, W. 2023 Nano-decolorization of methylene blue by *Phyllanthus reticulatus* iron nanoparticles: An eco-friendly synthesis and its antimicrobial, phytotoxicity study. *Applied Nanoscience* **13**, 2527–2537.

Elemike, E. E., Onwudiwe, D. C., Ekennia, A. C., Sonde, C. U. & Ehiri, R. C. 2017 Green synthesis of Ag/Ag_2O nanoparticles using aqueous leaf extract of *Eupatorium odoratum* and its antimicrobial and mosquito larvicidal activities. *Molecules* **22**(5), 674.

Elemike, E. E., Onwudiwe, D. C., Ekennia, A. C. & Jordaan, A. 2018 Synthesis and characterisation of silver nanoparticles using leaf extract of *Artemisia afra* and their in vitro antimicrobial and antioxidant activities. *IET Nanobiotechnology* **12**(6), 722–726.

Hussain, I., Singh, N. B., Singh, A., Singh, H. & Singh, S. C. 2016 Green synthesis of nanoparticles and its potential application. *Biotechnology Letters* **38**, 545–560.

Kumar, J. A., Krithiga, T., Manigandan, S., Sathish, S., Renita, A. A., Prakash, P., Prasad, B. S. N., Kumar, T. R. P., Rajasimman, M., Hosseini-Bandegharaei, A., Prabu, D. & Crispin, S. 2021 A focus to green synthesis of metal/metal based oxide

nanoparticles: Various mechanisms and applications towards ecological approach. *Journal of Cleaner Production* **324**, 129198.

Laouini, S. E., Bouafia, A., Soldatov, A. V., Algarni, H., Tedjani, M. L., Ali, G. A. M. & Barhoum, A. 2021 Green synthesized of Ag/Ag_2O nanoparticles using aqueous leaves extracts of *Phoenix dactylifera* L. and their azo dye photodegradation. *Membranes* **11**(7), 468.

Levard, C., Hotze, E. M., Lowry, G. V. & Brown Jr., G. E. 2012 Environmental transformations of silver nanoparticles: Impact on stability and toxicity. *Environmental Science & Technology* **46**(13), 6900–6914.

Mayuri, M., Asima, D. & Joseph, K. S. 2022 Phytochemical analysis and antioxidant activities of *Artemisia stelleriana* Besser leaf extracts. *Plant Science Today* **9**, 215–220. https://doi.org/10.14719/pst.1263.

Mittal, A. K., Kaler, A. & Banerjee, U. C. 2012 Free radical scavenging and antioxidant activity of silver nanoparticles synthesized from flower extract of *Rhododendron dauricum*. *Nano Biomedicine and Engineering* **4**(3), 118–124.

Mousavi, S. M., Hashemi, S. A., Ghasemi, Y., Atapour, A., Amani, A. M., Savar Dashtaki, A., Babapoor, A. & Arjmand, O. 2018 Green synthesis of silver nanoparticles toward bio and medical applications: review study. *Artificial cells, nanomedicine, and biotechnology* **46**, 855–872.

Prabhu, S. & Poulose, E. K. 2012 Silver nanoparticles: Mechanism of antimicrobial action, synthesis, medical applications, and toxicity effects. *International Nano Letters* **2**, 1–10.

Prasher, P. & Sharma, M., 2023 Chapter 15 – Mycogenic nanoparticles: Synthesis, risk assessment, safety, and regulation. In: *Fungal Cell Factories for Sustainable Nanomaterials Productions and Agricultural Applications. Nanobiotechnology for Plant Protection* (Abd-Elsalam, K. A., ed.). Elsevier, pp. 393–420. Available from: https://www.sciencedirect.com/science/article/pii/B9780323999229000209 (accessed 1 October 2023).

Puthukulangara Jaison, J. & Kadanthottu Sebastian, J. 2023 *Artemisia stelleriana*-mediated ZnO nanoparticles for textile dye treatment: A green and sustainable approach. *Water Practice and Technology* **18** (4), 911–921.

Ravichandran, V., Vasanthi, S., Shalini, S., Shah, S. A. A., Tripathy, M. & Paliwal, N. 2019 Green synthesis, characterization, antibacterial, antioxidant and photocatalytic activity of *Parkia speciosa* leaves extract mediated silver nanoparticles. *Results in Physics* **15**, 102565.

Rautela, A., Rani, J. & Debnath, M. 2019 Green synthesis of silver nanoparticles from Tectona grandis seeds extract: characterization and mechanism of antimicrobial action on different microorganisms. *Journal of Analytical Science and Technology* **10**, 5. doi: 10.1186/s40543-018-0163-z.

Shaikh, W. A., Chakraborty, S. & Islam, R. U. 2020 Photocatalytic degradation of rhodamine B under UV irradiation using *Shorea robusta* leaf extract-mediated bio-synthesized silver nanoparticles. *International Journal of Environmental Science and Technology* **17**(4), 2059–2072.

Sofowora, A., Ogunbodede, E. & Onayade, A. 2013 The role and place of medicinal plants in the strategies for disease prevention. *African Journal of Traditional, Complementary, and Alternative Medicines* **10**, 210–229.

Valappil, R. S. K., Ajuy, S. V. & Raj, M. B. 2019 Decolorization of Reactive Blue 220 aqueous solution using fungal synthesized Co_3O_4 nanoparticles. *Journal of Water Supply: Research and Technology – AQUA* **68**(8), 675–686.

Vijayakumar, M., Priya, K., Nancy, F. T., Noorlidah, A. & Ahmed, A. B. A. 2013 Biosynthesis, characterisation and anti-bacterial effect of plant-mediated silver nanoparticles using *Artemisia nilagirica*. *Industrial Crops and Products* **41**, 235–240.

Ying, S., Guan, Z., Ofoegbu, P. C., Clubb, P., Rico, C., He, F. & Hong, J. 2022 Green synthesis of nanoparticles: Current developments and limitations. *Environmental Technology & Innovation* **26**, 102336.

Zhang, Y., Cui, L., Lu, Y., He, J., Hussain, H., Xie, L. & … Wang, D. 2022 Characterization of silver nanoparticles synthesized by leaves of *Lonicera japonica* Thunb. *International Journal of Nanomedicine* **17**, 1647–1657.

First received 20 May 2023; accepted in revised form 16 October 2023. Available online 26 October 2023